

Kombinierte LIF und Filmdickenmessungen zur Untersuchung des Mischprozesses während des Tröpfchenaufpralls auf einen dünnen Flüssigkeitsfilm

Combined LIF and film thickness measurements to study the mixing process during droplet impact onto a thin liquid film

Hatim Ennayar*, Philipp Brockmann, Jeanette Hussong

Technical University of Darmstadt, Institut for Fluid Mechanics and Aerodynamics, Darmstadt, Germany

*ennayar@sla.tu-darmstadt.de

Tropfenaufprall, Dünne Filme, Mischen, Laserinduzierte Fluoreszenz

Drop Impact, Thin films, Mixing, Laser-induced-Fluorescence

Abstract

The present study focuses on combining laser induced fluorescence (LIF) and Film thickness measurements in order to develop an optical method determining the 2-dimensional (2D) local concentration during the mixing of a droplet into a thin liquid film. The use of a multidimensional calibration technique allows us to measure the local fluorescent concentration in a liquid film. Moreover, this technique permits the tracking of the film thickness variation for cases with known concentrations. A series of validation measurements were conducted to estimate the 2D local standard deviation of reconstructed concentration and film thickness. A quantitative investigation of the mixing of a droplet during impact onto thin fluid films of 200 μm and up to 800 μm is presented in the deposition regime. The effect of the fluid film thickness on the radial, instantaneous spreading and mixing of droplet liquid in the film is investigated gaining insights into the role of transient ring vortices during impact.

1 Introduction

The mixing process of droplets in thin liquid films is of great interest in various applications such as spray-coating and internal combustion engines (Yarin 2006). Ersoy and Eslamian 2019 investigated the mixing between droplet and film of same liquid during different impact regimes, where they showed how a decreasing film thickness results in a larger area of mixing for low energy impacts. The typical regimes during drop impact onto thin liquid film are droplet deposition, corona formation without splashing, corona formation with splashing and prompt splash. The resulting regime depends on the impact's energy and the ratio between film thickness and drop diameter $h^* = h/D_0$. The study of Chen et al. 2017, on the other hand, revealed the significant role of miscibility during drop impact onto thin film of different liquid. However, a quantitative description and understanding of the mixing process during the impact has not been conducted yet.

One challenge for a quantitative study of mixing is implementing a non-intrusive measurement technique enabling the extraction of 2D-concentration distributions. While shadowgraphic or

brightfield high-speed imaging is very effective for determining the geometrical deformations happening during the impact, they lack quantitative information about species transport. Other optical methods for inspecting impact phenomena such as Fourier transform profilometry (Lagubeau et al. 2017) and CHR sensor deployed by Van Hinsberg et al. 2010 were widely used. Another approach was performed by Hann et al. 2016. Here, the film thickness variations during drop impact onto thin films were measured by means of laser-induced fluorescence. Using a fluorescent dye as a label, their results showed great agreement with theoretical results. However, during mixing, the temporal and spatial dye concentration variation additionally affects the signal intensity during a LIF measurement (Shan et al. 2004). In the present study, local concentration changes in a rhodamine-B dyed water film during droplet impact is determined utilizing 2D1C Laser-induced-Fluorescence measurements. By combining LIF and thickness measurements with a confocal sensor, we are able to establish a multidimensional 2D calibration with respect to thickness, intensity and dye concentration which allows us to extract local concentration values during the impact.

Furthermore, we utilize our multidimensional calibration to extract the 2D local concentration of the fluid film during low energy impact (deposition regime). Three different cases consisting of 3 different film thicknesses ($h^* = 0.09, h^* = 0.22, h^* = 0.35$) are shown and discussed here.

2 Experimental Setup

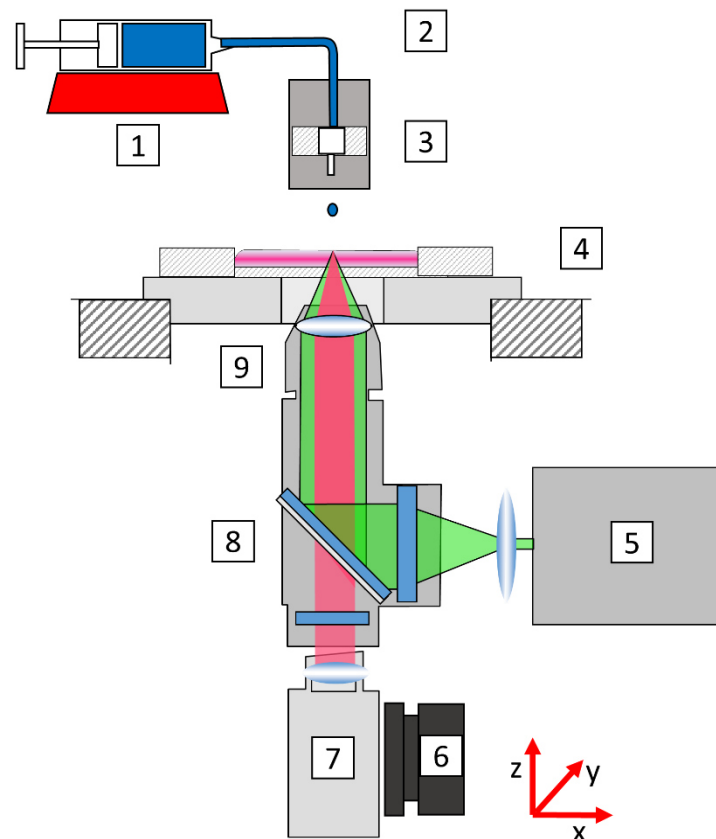


Fig. 1: Sketch of setup: 1) Syringe pump, 2) z-Traveler, 3) Cannula, 4) Thin liquid film on TFO glass substrate, 5) LED, 6) x,y,z-Traveler, 7) HS-Camera, 8) Dichroic mirror with band-pass filters, 9) Microscope.

Figure 1 shows a schematic sketch of the experimental setup. It consists of 3 principle parts. The drop generator system contains a syringe pump (Aladdin AL-1010, WPI), a 5ml syringe (Braun GmbH) and a cannula (Braun GmbH). The cannula is mounted on an automatically

controlled traverse for generating deionized water droplets ($\rho = 997 \frac{kg}{m^3}$, $\nu = 1.004 \cdot 10^{-6} m^2/s$, $\sigma = 72.25 mN/m$) with different impact velocities U . Deionized water dyed with rhodamine B (Carl Roth) is used to prepare the liquid film. With the means of a blade, thin liquid films are created on a fluorine doped tin oxide (FTO) coated substrate (Sigma Aldrich) of size 50 mm x 50 mm x 2.2 mm. The optical measurement part consists of a custom build microscope based on a tube (InfiniTube Special, Infinity Photo-Optical) illuminated with a 7W high power green chipped ($\lambda \approx 532 nm$) LED (ILA iLA.LPS v3). A filter cube (Thorlabs DFM1/M) containing a dichroic mirror and two band-pass filters enables directing the light through the objective and filters the fluorescence signal. The images are taken by a 12-bit, 1280x800 pixel CMOS high-speed camera (Phantom Miro Lab 110, Vision Research) with $20 \times 20 \mu m^2$ pixel size equipped with a microscope objective (IF-3, Infinity Photo-Optical) with 1X magnification and focal depth of 0.17 mm. The large value of focal depth permits the 2D investigation of concentration variations due to thin thicknesses. At a resolution of 512x512 pixel, the field of view is 8,25x8,25 mm² which allows capturing the whole impact. The optical system is mounted on a tridirectional traverse enabling the adjustment of its position for a perfect image recording.

3 Method and Calibration Procedure

For determining the local concentration during droplet impact by means of LIF measurements, it is necessary to establish first a multidimensional calibration method that takes into account all the parameters affecting the intensity of the fluorescence signal. The principle of the LIF technique is based on the Beer-Lambert law relating the emitted light to the local dye concentration. Moreover, the thickness of the fluid film directly affects the intensity of the signal as shown in eq. (1) (Alekseenko et al. 2008; Hann et al. 2016).

$$\frac{I(i,j) - D(i,j)}{C_M(i,j)} = [1 - e^{-\alpha \cdot h(i,j)}] \cdot [1 + k_{refl} \cdot e^{-\alpha \cdot h(i,j)}] \quad (1)$$

where I , D , C_M and h are the intensity of the fluorescence light, the black level of the camera, the compensation matrix, the local thickness of the film at each pixel (i,j) . k_{refl} represents the reflection coefficient of the water-air interface. In the present study, the coefficient of absorption of the dye α , is also varying during the droplet impact since the concentration of rhodamine B changes due to mixing.

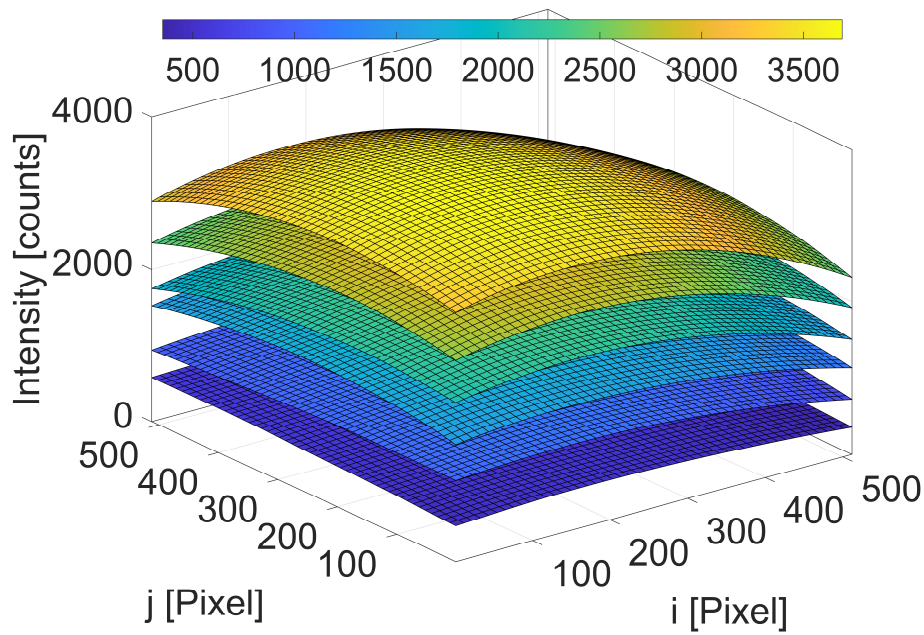


Fig. 2: Calibration surfaces of intensity distribution for 200 μm thin films with 6 different concentrations. From bottom to top: $1 \cdot 10^{-5}M$, $2 \cdot 10^{-5}M$, $4 \cdot 10^{-5}M$, $6 \cdot 10^{-5}M$, $8 \cdot 10^{-5}M$, $1 \cdot 10^{-4}M$.

The multidimensional calibration measurement is performed by taking multiple images of the fluid film with known thickness h and concentration C of the dye. The thin fluid film thickness ranges from 0 to 900 μm and rhodamine B concentrations in water are between 0 to 10^{-4} M (mol/L). The thickness of the fluid film is measured by a confocal sensor (confocalDT IFS2407-0,8, Micro-epsilon). A median filter with a kernel of $5px \times 5px$ is applied to the calibration images to reduce the noise, then a polynomial surface fit of degree 2 in i and degree 3 in j is applied to the intensity signal, where (i,j) is the pixel position as shown in figure 2. Another polynomial surface fit for the polynomial coefficients as function of h and C and of order 3×3 is then performed for each case with the goal to express the intensity signal in the following form:

$$I_{ij}(h(i,j), C(i,j)) = \sum_{k,l}^n a_{kl}(h(i,j), C(i,j)) \cdot i^k \cdot j^l \quad (2)$$

a_{kl} are the polynomial coefficients of the first surface fit and are function of the film thickness and the dye concentration.

4 Results

4.1 Validation measurements

For validating our calibration, multiple measurements were conducted to compare the measured dye concentration in the fluid film with the real concentration. Images were recorded for different thin liquid films of thickness and dye concentration ranging between 200 – 900 μm and $6 \cdot 10^{-6}$ – $8 \cdot 10^{-5}M$. The left graph in figure 3 shows that the measured concentrations are in great agreement with the real dye concentration. The plotted concentration is the mean value over the whole uniform film within the depicted field of view ($8.25 \times 8.25 \text{ mm}^2$). The reconstruction error of concentration is determined for each pixel. Figure 3 shows the instantaneous

relative error calculated by eq. (3). It ranges between 4% to 11%, excluding small areas where the error reach 14%. The median for all pixels has a value of 6.47%.

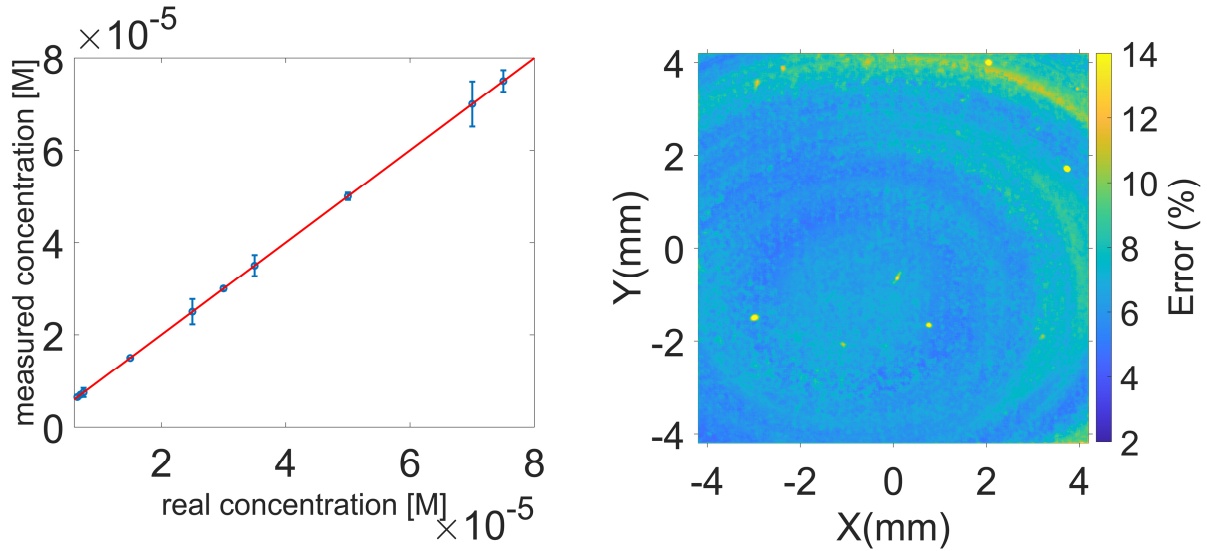


Fig. 3: Measured concentration for different uniform thicknesses (left), 2D local concentration error in each pixel for all validation measurements (right).

$$Error(i, j) = \frac{|C_{measured(i,j)} - C_{real}|}{C_{real}} \quad (2)$$

The error in the boundary top left is considerably higher due to the weakness of polynomial surface fitting on the boundaries. However, as the drop impact and mixing occur in the center region of the image, this large error does not compromise the measurement data.

4.2 Drop impact on thin film

Measurements of the droplet impact onto thin liquid film in deposition regime are performed. The water droplet has a diameter of $D = 2.15 \text{ mm}$ impacting on a film of three different thicknesses ($h^* = 0.09, h^* = 0.22, h^* = 0.35$) with a Reynolds number and Weber number of $Re = 3000$ and $We = 60$ respectively. The initial rhodamine B concentration in the thin film is $C_0 = 8 \cdot 10^{-5} M$. Figures 4a to 4e illustrate the droplet impact from a side view for a dimensionless thickness $h^* = 0.22$. The side view images are 10mm x 5mm. images taken with a frequency of 6 kHz of droplet impacting a thin liquid film of dimensionless thickness $h^* = 0.22$. Side view images were also recorded for a better understanding of the intensity signal variation during the impact. The X and Y position are normalized by the droplet diameter. Moreover, figure 4a ($t = 0 \text{ ms}$) is the first recorded image at which the droplet impacts the film.

When the droplet is in contact with the thin film (figure 4a,4f), an increase in the intensity signal is observed. This spike is mainly due to surface wave induced variations of the local film thickness. Afterwards, the spreading of the droplet generates a cavity with low signal intensity in the fluid film that can be clearly seen in figure 4g. Here the film thickness is significantly smaller compared to the initial value. Moreover, capillary waves can be seen visible through a high fluorescence signal. When the receding phase starts, some droplet liquid got entrapped in the maximum spreading radius of the lamella due to the clear decrease in the signal (figure 4h). This area will be called entrapment area where inertial mixing takes place. A small increase in

the signal intensity at $t = 16 \text{ ms}$ can be justified by the small rebound of the droplet during the receding phase. Finally, the thin liquid film transition back to a resting phase where it is well projected the change in signal intensity due to a change in local rhodamine B concentration (figure 4j). In this phase, film thickness measurements show a homogenous thickness such that signal variation solely emanate from concentration variation.

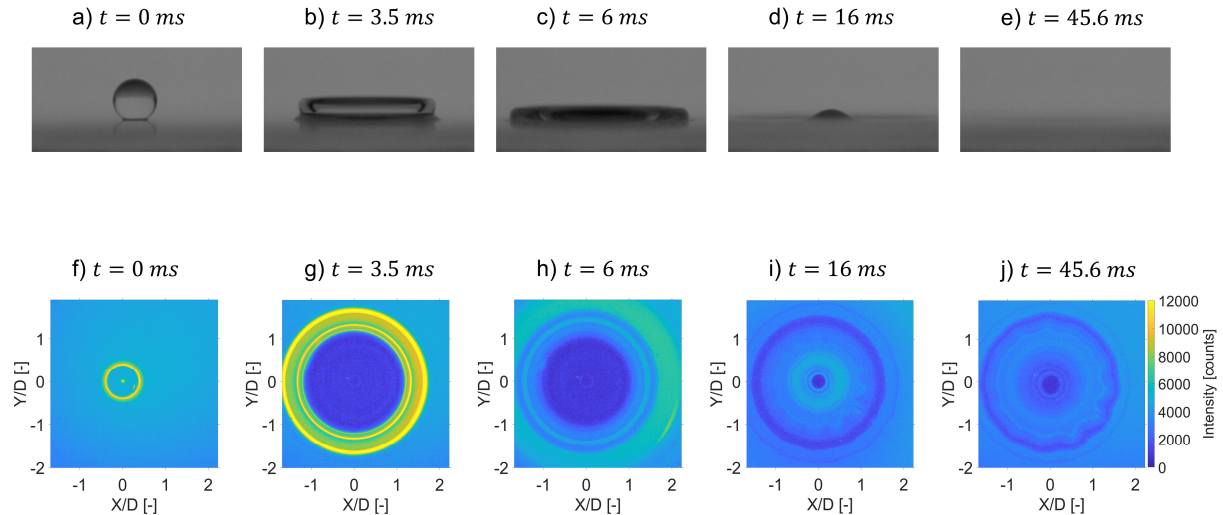


Fig. 4: Raw images of droplet impact onto thin liquid film at $We = 60$, $Re = 3000$ and $h^* = 0.22$. a) to e) represents the side view whereas f) to j) represents the bottom view.

Figure 5 shows the 2D local concentrations at $t = 45.6 \text{ ms}$ for three different film thicknesses. By using the multidimensional calibration and knowing the radial film thickness, the local concentration of rhodamine B after the impact is extracted. The results shown in figure 5 and 6 are then normalized by the initial concentration C_0 . Figure 6 illustrates the radial concentration deduced from figures 5a-5c. For all three thicknesses the lowest concentration of film dye is right in the centre of the impact where $C = 9.6 \cdot 10^{-6} M$. The concentration starts increasing gradually until it reaches circular ring where another dip in the concentration occurs. This circular ring differs from thickness to another. The ring is at maximum for thinner films as shown in figure 5a, and this is can be due to the acute angle of the lamella walls during the impact at low and moderate h^* and We as observed by **Fedorchenko and Wang 2004**.

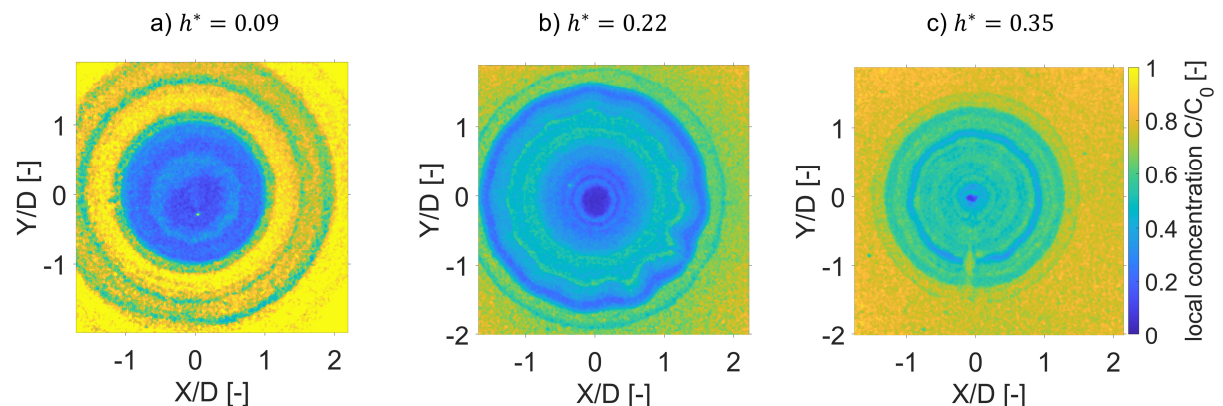


Fig. 5: 2D normalized local concentration of rhodamine B at $t = 45.6 \text{ ms}$ after the impact where $C_0 = 8 \cdot 10^{-5} M$ is the initial concentration. $We = 60$ and $Re = 3000$. The X and Y positions are normalized by the droplet diameter.

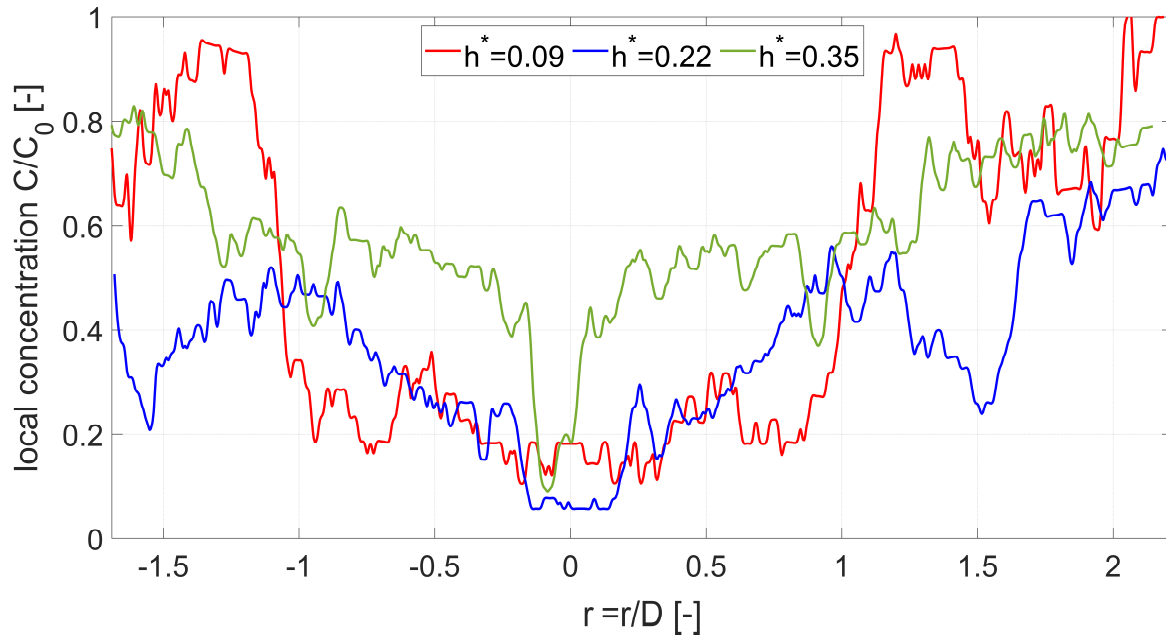


Fig. 6: 2D normalized radial concentration of rhodamine B at $t = 45.6 \text{ ms}$ after the impact where $C_0 = 8 \cdot 10^{-5} \text{ M}$ is the initial concentration. $We = 60$ and $Re = 3000$. The radial position is normalized by the droplet diameter.

The decrease in rhodamine b concentration in the circular ring area is mainly due to the existence of an inertial buffer zone (entrapment zone) where the droplet fluid is entrapped which leads to a better mixing. This entrapment occurs by means of ring vortices that enhance the mixing in that area. For extra thin films, which is the case of $h^* = 0.09$, the magnitude of the vortices is low which leads to a weak mixing in that area. Moreover, the majority of droplet fluid is then pulled back during the receding phase which explains the larger area of low rhodamine B concentration around the centre. On the other hand, the concentration of rhodamine B in the circular ring is much lower for thicker films.

A broad parameter investigation will be necessary to better understand the mechanism of mixing during droplet impact onto thin liquid films.

5 Conclusion and Outlook

In the present paper, a multidimensional calibration technique combining LIF and film thickness measurements is successfully conducted. This method allows to determine quantitatively the local concentration of the droplet in the liquid film during the mixing. Due to the short time scales, the study assumes that the rhodamine b dye is a passive tracer of the film liquid. While other LIF measurements focused only on measuring the thickness variation during droplet impact, this work was able to obtain not only thickness variations but also concentration variations. After validating the calibration technique, measurements were conducted to extract radial concentrations during droplet impact on three different films in the deposition regime. Moreover, 2D plots showed how the thickness of the fluid film affects the spreading and mixing of the droplet. A circular ring area containing the droplet liquid is formed at different radial position depending on the thickness of the film. This area which can be called the entrapment area seems to be an inertial dominated area with ring vortices that enhance the mixing process.

Acknowledgements

This project is funded by the Deutsche Forschungsgemeinschaft (DFG, German Research Foundation) – project number 237267381 – TRR 150, sub-project A07.

References

- Yarin, A.L., 2006** “Drop impact dynamics: Splashing, spreading, receding, bouncing...”. *Annu. Rev. Fluid Mech.* 38, 159
- Ersoy, N. E., & Eslamian, M. 2019.** Capillary surface wave formation and mixing of miscible liquids during droplet impact onto a liquid film. *Physics of Fluids*, 31(1), 012107
- Chen, N., Chen, H., Amirfazli, A. 2017** Drop impact onto a thin film: Miscibility effect. *Physics of Fluids*, 29, 092106
- Lagubeau, G., Fontelos, M.A., Josserand, C. et al. 2012** Spreading dynamics of drop impacts. *Journal of Fluid Mechanics*, 730:50-60
- Van Hinsberg, N.P., Budakli, M., Göhler, S. et al. 2010** Dynamics of the cavity and the surface film for impingements of single drops on liquid films of various thicknesses. *Journal of Colloid and Interface Science*, 350:336-343
- Hann, D.B., Cherdantsev, A.V., Mitchell, A. et al., 2016** A study of droplet impact on static films using the BB-LIF technique. *Experiments in Fluids* 57, 46
- Shan, J.W., Lang, D.B., Dimotakis, P.E. 2004** Scalar concentration measurements in liquid-phase flows with pulsed lasers. *Experiments in Fluids* 36, 268-273
- Alekseenko, S.V., Antipin, V.A., Cherdantsev, A.V. et al. 2008** Investigation of waves interaction in annular gas-liquid flow using high-speed fluorescent visualization technique. *Microgravity Science and Technology* 20:271-275
- Fedorchenko, A.I., Wang, A.B., 2004** On some common features of drop impact on liquid surfaces. *Physics of Fluids* 16, 1349